2012-01-01

Isotope Geochemistry and Geochronology of Lavas from the Line Islands Chain, Central Pacific Basin: Insight into the Origin of the Line Islands

Lauren Storm
University of Texas at El Paso, lpstorm@miners.utep.edu

ISOTOPE GEOCHEMISTRY AND GEOCHRONOLOGY OF LAVAS FROM THE LINE ISLANDS CHAIN, CENTRAL PACIFIC BASIN: INSIGHT INTO THE ORIGIN OF THE LINE ISLANDS

LAUREN PATRICE STORM

Department of Geological Sciences

APPROVED:

Jasper Konter , Ph.D., Chair

David Borrok, Ph.D.

Eric Hagedorn, Ph.D.

Benjamin C. Flores, Ph.D.
Interim Dean of the Graduate School

ISOTOPE GEOCHEMISTRY AND GEOCHRONOLOGY OF LAVAS FROM THE LINE ISLANDS CHAIN, CENTRAL PACIFIC BASIN: INSIGHT INTO THE ORIGIN OF THE LINE ISLANDS

by

LAUREN PATRICE STORM, B.S.

THESIS

Presented to the Faculty of the Graduate School of

The University of Texas at El Paso

in Partial Fulfillment

of the Requirements

for the Degree of

MASTER OF SCIENCE

Department of Geological Sciences

THE UNIVERSITY OF TEXAS AT EL PASO

August 2012

Acknowledgements

This work would not have been possible without the endless support of my committee members. First, I would like to thank Dr. Jasper Konter for introducing me to the geology that takes place in the Pacific Ocean. Without your endless time and knowledge, I would not have gained as much insight into the processes which take place in my research area. The resources used to conduct this research provided by Dr. Jasper Konter and Dr. David Borrok made this project possible. They went beyond their duty to properly educate me in using the laboratories and instrumentation needed for data collection. Dr. Eric Hagedorn had such enthusiasm towards geology that inspired me to continue on even if things were rough. He confirmed my decision in choosing geology after discussing his choice to come back as a geologist if he was reincarnated.

Also, I would like to thank my fellow colleagues who worked in the labs with me. They understood the concept of "late nights" when dealing with clean room separations, and how some days the mass spectrometer just doesn't like you. This company and friendship during long hours kept me sane.

Lastly, I am indebted to my parents and family for all of their love and support during these past two years. Not only did you teach me to work hard, but you also instilled in me the desire to achieve and do my best in all that I do. Although you didn't want to see your "little girl" leave home, you allowed me to acquire my goals, and with that I thank you.

Abstract

Geochemical compositions of melts produced in the Earth's mantle provide key data for understanding Earth's internal structure. Particularly, the compositions of unusually large outpourings of basaltic lavas in large igneous provinces involve substantial source volumes, thereby contributing to our understanding of mantle structure and dynamics. Although the origin of such lavas remains enigmatic, geochemically they may originate from Earth's oldest and deepest mantle reservoir, transported by a mantle plume or by entrainment in passive upwelling beneath a fast spreading center. The Pacific Ocean basin hosts several large igneous provinces that formed near a triple junction of three oceanic plates, and we here focus on the coupled Mid-Pacific Mountains-Line Islands system of a large igneous province and a linear volcanic chain. Our new Sr-Nd-Pb isotope and $^{40}Ar/^{39}Ar$ data show complex age relationships along these volcanic structures, and a Pb isotope anomaly that is found in a cluster of small and distinct volcanoes that are geographically grouped. The geographical distinction relates to the plate tectonic structure of the area, limited to the north and south by fracture zones that bounded a captured Pacific microplate. We argue here that very high mantle flow beneath the triple junctions during the highly active Cretaceous period may have sampled dense material from the top of the Pacific large low shear velocity province. Delamination of this dense material and associated mantle influx could generate later, smaller-scale volcanism with a distinct composition and with complex age relationships.

Table of Contents

List of Figures

Chapter 1: The Line Islands-Mid Pacific Mountain LIP System

1.1 Introduction

Regionally extensive and voluminous mid-Cretaceous intraplate volcanism are products seen throughout much of the western and central Pacific Ocean basin (Winterer, 1973; Watts et al, 1980; Schlanger et al, 1981). Linear island chains, groups of seamounts and submarine plateaus represent this major volcanic activity (Floyd, 1989). These plateaus are known as large igneous provinces (LIPs), and the relationship of LIPs and linear volcanic chains has been explained as the volcanism of a mantle plume head (LIP) followed by volcanism by the plume tail (linear chain). The distribution of LIPs on the surface is thought to be an expression of deep mantle structure. More specifically, the mantle source for LIPs may be rooted in the large low shear velocity provinces (LLSVPs; Torsvik et al, 2008), and the volcanic systems considered here are examples of this relationship in the Pacific Ocean basin (Figure 1; Wessel et al, 2008). In addition to representing deep mantle structure, LIPs and volcanic chains have been used to model "absolute" Pacific plate motion over an assumed fixed plume source (e.g. Wessel et al, 2008).

LIP and ocean island basalt (OIB) compositions have also been used to study deep mantle processes. OIBs provide some of the only samples from the deeper mantle, and their rather variable radiogenic isotope compositions suggest that they have distinct origins within the mantle (e.g. Hofmann, 2003). The variability is thought to be caused by the incorporation of subduction-recycled material into the mantle that has remained after early extraction of the Earth's crust. Observed compositions are typically explained by mantle plumes returning mixtures of the mantle materials to the bottom of the lithosphere , where they melt by decompression (e.g. Hofmann, 2003). The potential survival of very early formed mantle reservoirs is a commonly discussed topic in the light of observed mixing trends (e.g. Zindler and Hart, 1986). Recent work using the now extinct ^{146}Sm-^{142}Nd system has led to a proposal of a mantle-scale fractionation event to explain the difference between Earth's mantle and meteorites that occurred within the first few hundred Ma of Earth's history (Boyet and Carlson, 2010). This model requires a "hidden" reservoir, and it was recently proposed that several Pacific Ocean LIPs

have isotopic ratios resembling such a primitive reservoir, suggesting that they may sample such material (Jackson and Carlson, 2011).

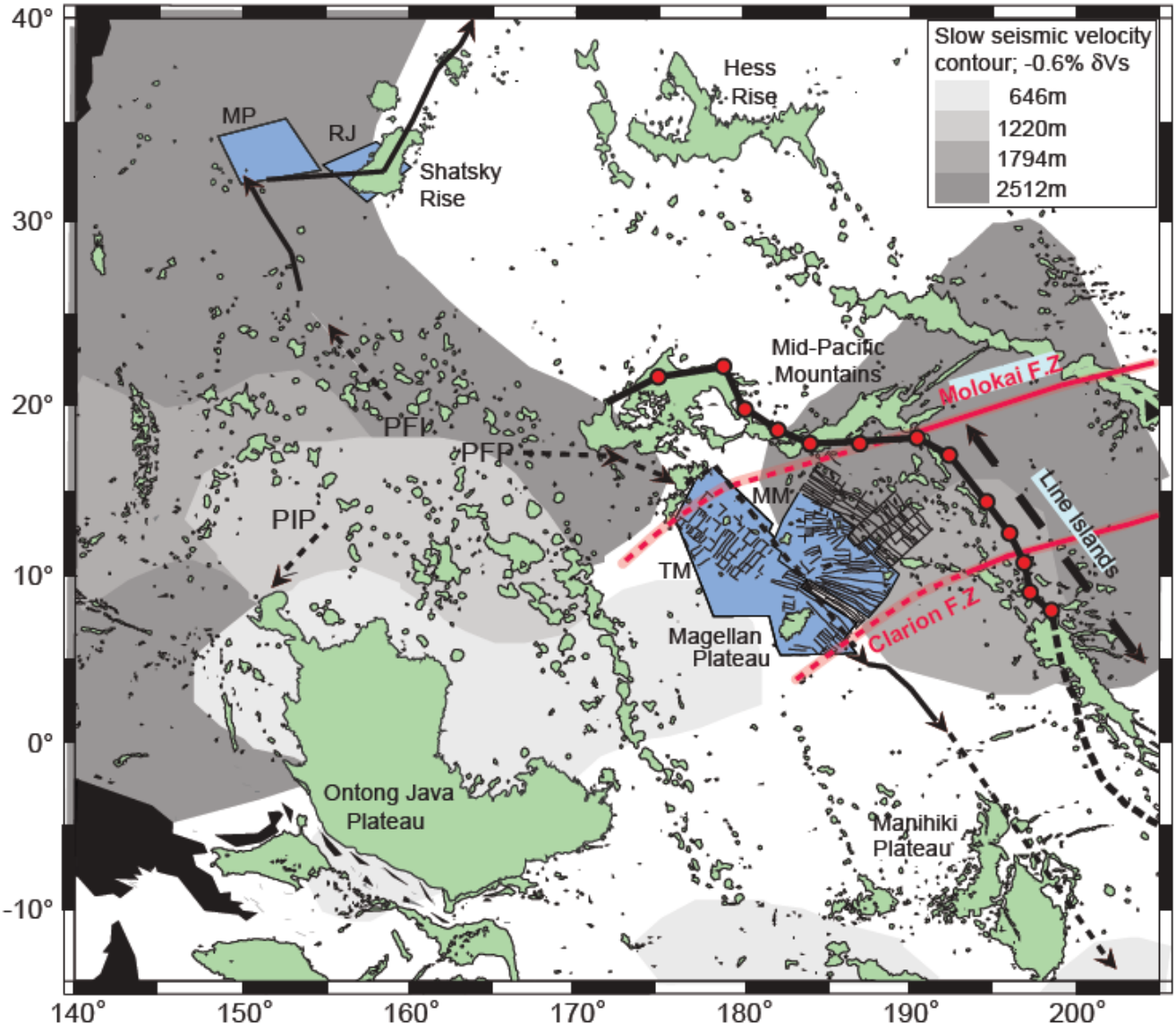

Figure 1: Regional locality map of the Line Islands showing Mesozoic microplates and plateaus, modified from Sager (2005). Thin solid lines are magnetic lineations corresponding to the Trinidad microplate (TM) and the Magellan microplate (MM). Heavy solid and dashed lines show the migration of the triple junctions. The predicted track for the Line Islands is represented with a solid black line and red dots. Dashed line extending from the reconstruction connects extinct volcanoes to the assumed seamount chain (modified from Wessel and Kroenke, 2008). S-wave velocity anomalies (SMEAN; Becker and Boschi, 2002) were compared at four different depths from the location of the original eruption of Shatsky Rise and the Mid-Pacific Mountains. PIP, Pacific- Izanagi-Phoenix triple junction; PFI, Pacific-Farallon-Izanagi triple junction; PFP, Pacific-Farallon-Phoenix triple junction; RJ- Ridge Jump; MP- Unnamed microplate.

As an alternative to a plume origin for LIPs, Korenaga (2005) proposed entrainment of dense fertile material into mantle flow related to rapid seafloor spreading, in order to satisfy first order geophysical observations. The dense material may originate from the subducted oceanic crust that is delaminated and fragments may become entrained at, for example, the 660 km seismic discontinuity, where the dense material might pond. Although fast seafloor spreading may be sufficient to entrain subducted material (Korenaga, 2005), the isotopic composition of LIPs, as described by Jackson and Carlson (2011), does not suggest an origin in subducted materials. Therefore, the mantle plume model may fit the isotopic data better, while the passive flow model explains other geophysical observations.

Here we focus on the coupled Mid-Pacific Mountains-Line Islands system of a LIP and a linear volcanic chain to test these models. New $^{40}Ar/^{39}Ar$ dates allow for unique insights into the origin of the Line Islands, however, the complexity in acquired age data requires geochemical compositions to evaluate further relationships of different mantle processes. We assess Sr-Nd-Pb radiogenic isotope compositions and age relations, and we use a localized Pb isotope anomaly to suggest how the Line Islands evolved, combining components from both the plume model and passive flow model.

1.2 Background and Sample Description

The configuration and tectonic history of four plates in the Pacific Ocean basin has been described in detail by Nakanishi and Sager (1996) and Nakinishi (1991). In association with the spreading of the Pacific, Farallon, Izanagi and Phoenix plates, three major Mesozoic magnetic anomaly lineation sets were formed in the NW Pacific Ocean. These indicate that the Pacific plate was bounded by three ridges, namely the Pacific-Izanagi ridge, the Pacific-Farallon ridge and the Pacific-Phoenix ridge. There are also two minor lineation sets, the Magellan and Mid-Pacific Mountains sets that are related to activity of the Magellan microplate, near the Line Islands-Mid Pacific Mountain system. Nakanishi et al. (1989) described the configuration and tectonic history of the Pacific-Izanagi-Farallon triple junction to be a ridge-ridge-ridge (RRR) junction, yet the tectonic history of the Pacific-Farallon-Phoenix triple junction was inconclusive due to unidentified magnetic anomaly lineations from chron M20-M14. After the birth of the Pacific plate (192 Ma) until chron M22 (149 Ma), the configuration of

the triple junction was a fault-fault-ridge (FFR) junction, and after chron M9 (129 Ma), it was a RRR junction. Between chrons M15-M9, the Magellan microplate was active near the triple junction (Tamaki and Larson, 1988; Nakanishi and Winterer, 1998).

The Line Islands volcanic chain and Mid-Pacific Mountains lie adjacent to the former triple junction (Figure 1). The Line Islands were constructed on ocean crust that was erupted during the Cretaceous Normal Superchron, therefore lacking magnetic lineations and a related tectonic reconstruction. Morphologically, there are three distinct regions in the Line Islands, each has been intersected by the Line Islands Cross Trend with en echelon ridges (Winterer, 1976). The northern province between the Molokai and Clarion fracture zones consists of smaller volcanic structures, while the central and southern islands provinces contain immense and voluminous outpourings of lava.

The petrology of basalts from the Line Islands is similar to other mid-plate island chains (Jackson et al, 1976). Basalts range in composition between Hawaiian tholeiitic and alkali lavas, with particularly hawaiites, phonolites and potassic nephelinites. Previously determined isotopic compositions overlap with data trends for many other mid-plate island chains (FOZO; FOcal ZOne; Hart et al, 1992) and the enriched end of mid-ocean ridge basalts (C; Common Component; Hanan and Graham, 1996). Previously collected data for the Line Islands suggest relatively low $^{87}Sr/^{86}Sr$ ratios, although not uncommon for oceanic island basalts (Garcia et al, 1993).

1.3 $^{40}Ar/^{39}Ar$ Dating and Age Progressions

$^{40}Ar/^{39}Ar$ ages were obtained from 34 samples on leached groundmass and plagioclase, hornblende and biotite separates. Resulting ages range from 36.2 Ma to 98 Ma and seem to follow an overall linear trend when compared to the location of each sample (Figure 2). The oldest samples recorded are seen at the north end of the chain and the youngest samples are at the southern end, yet there is much variability along the entire length of the chain. Although this coarse-scale age progressive trend implies a hotspot origin, the significant scatter of age versus location along the chain suggests that a single hotspot track could not have formed the Line Islands (Figure 2).

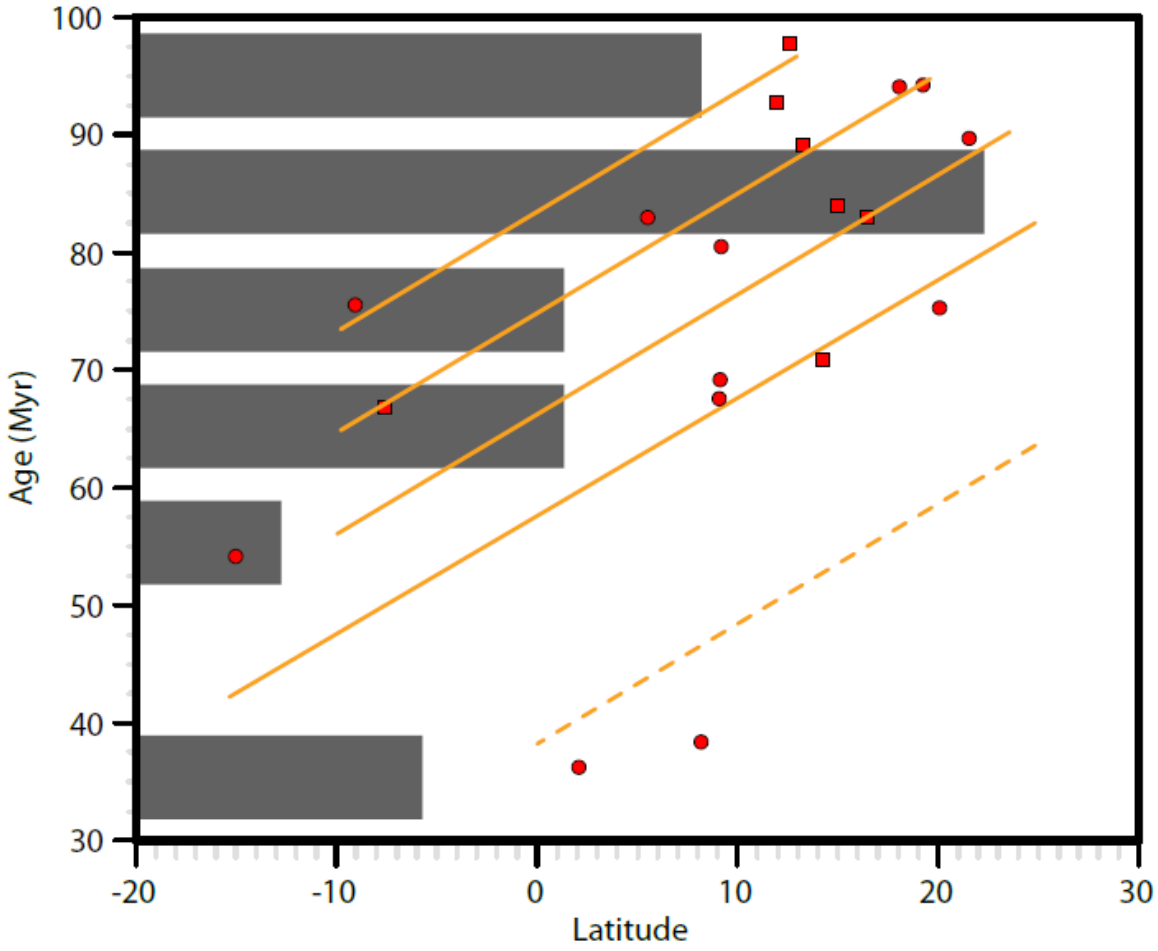

Figure 2: Volcano ages versus location (latitude). Wide scatter of data may result from multiple plume-fed hotspots, generating parallel slopes (orange lines), or arbitrary volcanic activity along the island chain at several different times (grey bars). Samples representing high $^{206}Pb/^{204}Pb$ ratios are shown with red boxes.

Since complex age relationships do not fit a simple plume-generated hotspot, other models should be evaluated. The currently available age data can be interpreted as either widespread volcanism along the entire chain during multiple time spans in geologic history, or overlapping volcanic chains resulting from multiple hotspots. If volcanism actively erupted along the entire chain during particular intervals in history, then a non-plume origin would be suggested, particularly if the volcanoes are compositionally distinct during each time period. Alternatively, if multiple age progressions can be recognized that are compositionally consistent along each volcanic chain, multiple plume-fed hotspots may have constructed one long and complex volcanic chain.

Geochemical data can help distinguish between these two possibilities. One would expect consistent geochemical compositions within each required hotpot chain if indeed the Line Islands follows a multiple plume model (e.g. Konter et al, 2008). If plume-fed hotspots are not the cause, then age progressive groups of volcanoes within the Line Islands are not necessarily associated with the same mantle source and may have different compositions.

1.4 Isotopes and Geographical Distribution

Twenty new Sr, Pb and Nd isotope ratio analyses of samples define two distinct compositional groups that both occur along the entire length of the seamount chain. $^{143}Nd/^{144}Nd$ ratios range from 0.512746-0.513002, while most of the leached lavas have low $^{87}Sr/^{86}Sr$ ratios (0.702986-0.703851), except for two samples (Lin 23, 0.704312; Lin 32, 0.704610). Garcia et al, (1993) already pointed out that the $^{206}Pb/^{204}Pb$ isotope data for the Line Islands are similar to several south Pacific oceanic island chains such as the Louisville Ridge, Marquesas, Easter, and Sala y Gomez. However, we recognize two groups of samples within the Line Islands: 1.) a group with intermediate $^{206}Pb/^{204}Pb$ ratios from 18.747-19.472, sampled from large volcanic structures north of the Molokai and south of the Clarion fracture zones, and 2.) a group with higher $^{206}Pb/^{204}Pb$ ratios than the rest of the Line Islands (19.788-20.149; Figure 3), although they do not stand out in any other compositional parameters. The second group consists of mainly small volcanoes, spatially limited between the Molokai and Clarion fracture zones. Moreover, this geochemical distinction cannot be related to any type of age progression.

The combination of relatively high $^{206}Pb/^{204}Pb$, and low to moderate $^{87}Sr/^{86}Sr$ and $^{143}Nd/^{144}Nd$ ratios cause the Line Islands to overlap with FOZO, C and Prevalent Mantle (PREMA) and range toward HIMU (Zindler and Hart, 1986; Hart et al, 1992; Hanan and Graham, 1996). It should be pointed out that the most recent composition suggested for FOZO provides a greater overlap than older definitions (Hart et al, 1992; Hauri et al, 1994; Stracke et al, 2005). Furthermore, it was recently pointed out that several LIPs resemble PREMA in composition (Jackson and Carlson, 2011), and we here assess such a fit and its implications for the origin of the Line Islands.

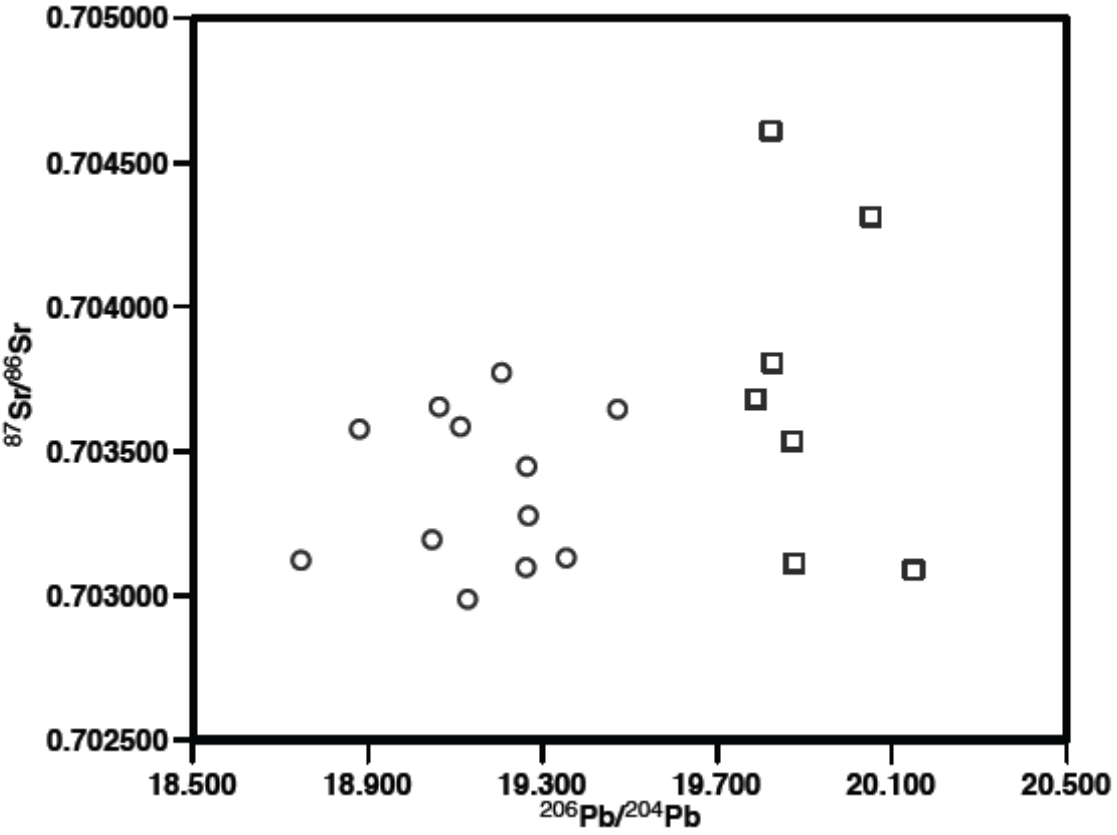

Figure 3: $^{87}Sr/^{86}Sr$ versus $^{206}Pb/^{204}Pb$ isotope ratios measured on the Nu Plasma MC-ICP-MS at UTEP. Circles represent samples located north of the Molokai fracture zone and south of the Clarion fracture zone. Samples that are geomorphologically controlled lie within the Molokai and Clarion fractures zones (squares).

1.5 Evolution of the Line Islands

Major LIPs have isotopic compositions near what is expected for the non-chondritic primitive reservoir that is implied by ^{146}Sm-^{142}Nd data, suggesting that they may sample relatively pristine mantle (Jackson and Carlson, 2011). Although current distributions of non-chondritic primitive material is not known accurately, palaeo-geographic relationships between LIPs and LLSVPs have shown that most LIPs erupted over one of two LLSVPs; one beneath Africa and one beneath the Pacific (Torsvik et al, 2008). Although mainly focusing on Atlantic hotspots, Torsvik et al. (2008) suggest that the Pacific and African LLVSPs have remained stationary in the mantle for up to 540 Ma. Given this stability and their composition reflected in LIPs, these structures may host a primitive non-chondritic mantle reservoir. The Line Islands-Mid Pacific Mountains overall have similar compositions to other LIPs, and a

reconstruction of their original eruptive location (Wessel and Kroenke, 2008) places this system in an area currently underlain by the Pacific LLSVP (Figure 1).

The magnetic lineations that define the Magellan microplate near the Line Islands-Mid Pacific Mountains system also show that the larger volcanic structures of this system erupted near the northern and southern end of the microplate (Figure 1). The microplate lineations are bounded by transform faults that roughly align with the Molokai and Clarion fracture zones. The volcanic system north and south of the microplate is morphologically larger than the seamounts in between the fracture zones. This difference is likely related to the different source and origin of these volcanoes, as implied by their distinct $^{206}Pb/^{204}Pb$ compositions. The lack of a simple age progression and the spatial distinction in composition lead us to explore the non-plume model of Korenaga (2005) as an explanation for the Line Island-Mid Pacific Mountain system.

The LIP model of Korenaga (2005) aims to explain the unexpectedly deep eruption of the Ontong-Java Plateau, while its current depth is too shallow for the eruption volumes expected from a plume. Korenaga (2005) suggests that melting of fertile material, included as dense blocks in passive flow under mid-oceanic ridges, may explain the observations. This model assumes that fast upwelling velocities overcome slow sinking of the dense material, until the material passed through the melting, where the vertical mantle flow decreases and the material may start sinking or delaminating. Inflow of upper mantle material that takes its place may then cause a later pulse in decompression melting and magmatism.

We here extend the model proposed by Korenaga (2005) to the Line Islands-Mid Pacific Mountains. As noted by Sager (2005), this LIP erupted near a triple junction just like the Ontong-Java Plateau and Shatsky Rise. We expect this to have focused relatively fast Cretaceous spreading and related mantle flow in a small area. The mantle material that was sampled by these LIPs, when their original eruptive location is approximately reconstructed (Figure 1; also following Torsvik et al, 2008), was sourced from near the edge of the Pacific LLSVP. The LLSVPs are thought to be stable or very slow moving structures (Torsvik et al, 2008; Schubert et al, 2004), agreeing with the composition of the Ontong-Java Plateau matching that of a proposed primitive reservoir that overlaps PREMA (Jackson and

Carlson, 2011). A similar composition may be sampled by the larger volcanic structures of the Line Islands-Mid Pacific Mountains, since their compositions overlap with the Ontong-Java Plateau. Following Korenaga (2005), these larger volcanic structures may result from fast passive flow, including fertile material from near the 660km discontinuity, producing large amounts of melt. If the Pacific LLSVP reaches to the transition zone, it may be contributing fertile material to the passive flow regime, explaining both the primitive compositions and the thickness and depth of eruption arguments for LIPs.

Renewed volcanism after the main LIP eruption was explained by Korenaga (2005) by delamination of the melted dense, fertile material, allowing upper mantle material to take its place, thereby decompressing and melting. This process should occur within ten to several tens of Ma, and such volcanism would be expected to produce minor volumes, and be different in compositions. These expectations match well with the smaller volume volcanoes between the Molokai and Clarion fracture zones, which are also isotopically different than the larger volcanic structures. More importantly, their higher $^{206}Pb/^{204}Pb$ is within the range of mid-ocean ridge basalt (ranging to C or FOZO; Hart et al, 1992; Hanan and Graham, 1996), therefore in agreement with the upper mantle source that would take the place of delaminating material.

Another aspect that may be explained with this model is the mismatch of the Line Islands chain with predicted plate motion (Wessel et al, 2008). Steinberger's (2000) mantle flow model predicts mantle flow to the northeast, which would push mantle source material away from what would be a "fixed" transition zone source, creating a volcanic chain progressively displaced from its expected track. Furthermore, only a coarse-scale age-progression would be expected, since plate tectonic motion, upper mantle motion and individual delamination events would determine where activity might take place next. Therefore, the changes seen in Pb isotope signatures and the lack of a detailed age progression throughout the Line Islands likely signify differences between LLSVP and upper mantle sampling.

This text, in full, will be submitted to the journal *Geology*, Storm, L.P., Konter, J.G., and Koppers, A.A.P., 2012.

Chapter 2: Techniques

2.1 Geochronology and Geochemistry

2.1.1 Samples and Methods

To test our hypotheses, a suite of 20 samples were prepared for geochemical analysis. To minimize the effect of seawater alteration, only the freshest material from each of the two cores was crushed, washed with 18MΩ water then dried, and hand-picked. Along with Site 315 core, another twenty samples, previously leached and analyzed for $^{40}Ar/^{39}Ar$ age dates at Oregon State University, were weighed (~200mg) and again leached with 6M HCl. After leaching, the samples were rinsed with double-distilled quartz water, and then dissolved using concentrated double-distilled HNO_3 and Fisher OPTIMA Grade HF. Samples were subsequently treated with concentrated double-distilled HNO_3 and double-distilled ~4M HCl to obtain the clearest possible sample solutions. Lastly, each sample was dried before being prepared for column separations. All column separations were carried out with double-distilled acids and Fisher OPTIMA Grade HF. The separations for Sr-Pb-Nd were all carried out on a single dissolution for each sample. In short, we modified techniques from Pin and Zalduegui (1997), Deniel and Pin (2001), and Rodriguez et al. (2007) to perform separations using Eichrom Sr-resin, TRU-resin, and LN-resin columns, as well as small AG1-x8 and AG50-x8 columns.

2.1.2 Strontium

Following Deniel and Pin (2001), and Rodriguez et al. (2007), the entire sample was passed through a Sr-resin column, separately collecting a Sr and Pb fraction, while Nd is eluted with the major elements. In detail, precleaned Sr-resin (250 µl resin bed; 100-150 mesh) was washed with 6M HCl and Q H_2O, then conditioned with 3M HNO_3 before loading the sample. Each sample was loaded onto the column in 6 column volumes (c.v.) 3M HNO_3, after refluxing overnight. First, the matrix is collected (including Nd) by rinsing with 3M HNO_3. Strontium was collected in 4 c.v. H_2O. Lead was subsequently eluted with 15 c.v. 6M HCl. To improve the purity of the Sr and Pb fractions, the Sr was passed through Sr-resin a second time, while Pb was passed through a different column.

2.1.3 Lead

In order to improve the purity of the Pb fraction, the collected Pb was passed through an AG1-x8 (250µl resin bed; 100-200 mesh) column, using HBr-HCl chemistry (e.g. Hanan and Schilling, 1989). Precleaned resin was washed with H_2O and 6M HCl and conditioned with 1M HBr. Samples were refluxed in 1M HBr and then loaded on the columns. The samples were then rinsed with 5 c.v. 1M HBr and 2M HCl, and subsequently, lead was eluted in 6M HCl.

2.1.4 Neodymium

The REE and matrix fraction that was collected during the Sr and Pb separation was used for the Nd procedure, using a technique modified from Pin and Zalduegui (1997). The solution was first dried down, then refluxed in 4mL 0.2M HNO_3. Subsequently, ~200mg of ascorbic acid (powder form) was added to reduce all Fe^{3+} to Fe^{2+}, such that only a small TRU-resin column (0.5 ml; 100-150 mesh) is needed to perform the separation of REEs from matrix elements (Horwitz et al., 1994). Compared to Pin and Zalduegui (1997) we have lowered the concentration of the HNO_3 acid, and combined with the use of ascorbic acid, this approach does not require pretreatment with an AG1-x8 resin column to remove Fe. Before loading onto the TRU-resin, the samples were centrifuged and the column was rinsed with 0.2M HNO_3 and the matrix, was collected in 8 c.v. The LREE's were then eluted in 8 c.v. 0.05M HNO_3. The collected LREEs were then passed through a different column to separate the Nd.

Nd separation was performed using LN-spec resin (1.7 ml; 50-100 mesh), following Hanan et al. (2004; 2008). The LREE fraction was dried, then converted to HCl. Columns were cleaned with a reservoir volume (15mL) of 0.18M HCl to strip the resin from any previous use. The samples were poured directly into the reservoir in 3.5 c.v. 0.18M HCl. The resin was then rinsed with 11 c.v. 0.18M HCl before eluting the Nd in 8 c.v. 0.18M HCl.

2.2 Mass Spectrometry

Mass spectrometric analysis was carried out by MC-ICP-MS on the Nu Plasma HR at the University of Texas at El Paso (UTEP) for Sr, Pb, and Nd. To monitor machine performance on the MC-ICP-MS, standards were run systematically after every two samples. Samples were highly diluted

in 0.05M HNO_3 to check their concentrations, then a sample solution was used matching the standard signal intensity within 10%.

Sr was measured on the MC-ICP-MS in multi-dynamic wet mode, correcting for isobaric interferences from ^{87}Rb, ^{84}Kr and ^{86}Kr. We have found that an internal correction for Kr interference on ^{86}Sr yields more precise data than an on-peak-zeroes subtraction. The UTEP Sr routine uses ^{84}Kr for the Kr correction on ^{86}Kr, after deconvolving the ^{84}Kr from the ^{84}Sr intensity. This approach yields better results than using one of the minor Kr isotopes (^{82}Kr, ^{83}Kr), which cannot accurately be determined due to their low signal levels. Such low signals result in significant error propagation into estimates of ^{86}Kr. Therefore, we measure the signals at both masses 84 and 86 with respect to the non-interfered ^{88}Sr. These masses contain contributions from both Sr and Kr, and we use the fact that ^{84}Sr, ^{86}Sr, ^{88}Sr ^{84}Kr, and ^{86}Kr are stable isotopes. Therefore, the signal at mass 84 (and similarly, mass 86) can be written as:

$^{84}Sr\ (V) = Total84\ (V) - {}^{84}Kr\ (V)$

When measured with respect to ^{88}Sr, mass fractionation of the MC-ICP-MS also has to be accounted for. The Kr interference constitutes <10mV of the total signal, while Faraday (Johnson) noise is roughly 20μV (Nu Plasma specifications for 10 second integration). This suggests Kr can only be characterized to about 3 significant figures. Given its simplicity, we use the power law to correct for mass fractionation during the interference correction only, and assuming that mass fractionation of Sr and Kr is similar for the purpose of the Kr correction, we can write:

$$f = \left[\left(\frac{^{84}Sr}{^{88}Sr}\right)_{True}\Big/\left(\frac{^{84}Total - {}^{84}Kr}{^{88}Sr}\right)_{Meas} - 1\right]/4$$

and

$$f = \left[\left(\frac{^{86}Sr}{^{88}Sr}\right)_{True}\Big/\left(\frac{^{86}Total - \left(^{84}Kr/\left(^{84}Kr/^{86}Kr\right)_{Known}\right)}{^{88}Sr}\right)_{Meas} - 1\right]/2$$

which represent two equations with two unknowns (f and ^{84}Kr), using a known (measured) $^{84}Kr/^{86}Kr$ ratio. We used Matlab to solve for f and ^{84}Kr and apply this solution online, where we can then calculate the ^{86}Kr contribution and calculate a corrected ^{86}Sr value. Next, we correct ^{87}Sr for the isobaric interference from ^{87}Rb by monitoring ^{85}Rb. Finally, $^{87}Sr/^{86}Sr$ is calculated using the exponential law relative to the Kr-corrected ratio $^{88}Sr/^{86}Sr = 0.1194$. We have assessed the effect of our assumptions (power law approximation and a "known" $^{84}Kr/^{86}Kr$ ratio for the Kr correction) and found that both assumptions only affect the data in about the seventh digit of the $^{87}Sr/^{86}Sr$ ratio. For example, the "known" $^{84}Kr/^{86}Kr$ ratio can be adjusted from a measured ratio to the "true" ratio without affecting the $^{87}Sr/^{86}Sr$ ratio. Furthermore we compared our calculated ^{84}Kr to an on-peak-zeroes measurement and obtained values within error, suggesting the overall approach adequately decovolves the Sr interference. Using this approach, NIST SRM 987 averaged 0.710231 ±9 (2 $\sigma/\sqrt{n}$) over the period over which the measurements were made. All data were normalized to NIST SRM 987 = 0.710248, using the daily average for that standard. The reported uncertainties of the data represent in-run precision.

The Pb isotopic analyses were carried out in dry mode (DSN-100) by Tl doping (NIST SRM 997 Tl and $^{205}Tl/^{203}$ Tl= 2.3889; White et al. 2000; Hanan et al., 2004; 2008), bracketing NIST SRM 981 to correct for mass fractionation and machine bias (White et al., 2000). Bracketing NIST SRM 981 values were adjusted to accepted values (Todt et al., 1996). The standard NIST SRM 981 averaged $^{206}Pb/^{204}Pb = 16.934 \pm 4$, $^{207}Pb/^{204}Pb = 15.489 \pm 5$, and $^{208}Pb/^{204}Pb = 36.689 \pm 15$ (2 $\sigma/\sqrt{n}$) over an extended period, whereas averages of individual sessions have 2 $\sigma/\sqrt{n}$ of <0.001 for $^{206}Pb/^{204}Pb$ and $^{207}Pb/^{204}Pb$, and <0.002 for $^{208}Pb/^{204}Pb$. The reported uncertainties of the data represent in-run precision.

Neodymium was measured following Hanan et al. (2004; 2008) in dry mode (DSN-100). Nd isotope data were collected using multi-dynamic mode, and data were corrected for mass fractionation by normalizing to $^{146}Nd/^{144}Nd = 0.7219$ using an exponential law. The NJdi-1 standard is run on a daily basis as the bracketing standard, and it averaged $^{143}Nd/^{144}Nd = 0.512083 \pm 4$ (2 $\sigma/\sqrt{n}$) over this period, while La Jolla Nd average 0.511839 ±3 (2 $\sigma/\sqrt{n}$). Uncertainty on Nd isotope ratios are 2 $\sigma/\sqrt{n}$ of internal run statistics.

References

Becker, T. W., and L. Boschi, 2002. A comparison of tomographic and geodynamic mantle models, Geochem. Geophys. Geosyst., *3,* 10.129/2001GC000168, 2002.

Boyet, M., Carlson, R.W., and Horan, M., Old Sm-Nd ages for cumulate eucrites and redetermination of the solar system initial $^{146}Sm/^{144}Sm$ ratio, *Earth Planet. Sci. Lett.,* 291, 172-181, 2010.

Deniel, C., and Pin, C., Single-stage method for the simultaneous isolation of lead and strontium from silicate samples for isotopic measurements, *Analytica Chimica Acta*, 426, 95-103, 2001.

Floyd, P.A., Geochemical features of intraplate oceanic plateau basalts, *Geol. Society, London, Special Publications,* 42, 215-230, 1989.

Garcia, M.O., K.H. Park, Davis, G.T., Staudigel, H., and Mattey, D.P., Petrology and isotope geochemistry of lavas from the Line Islands chain, central Pacific Basin, *The Mesozoic Pacific: Geology, Tectonics and Volcanism, Geophys. Monogr.,* 77, 217-231, 1993.

Hart, S.R., E.H. Hauri, L.A. Oschmann, and J.A. Whitehead, Mantle plumes and entrainment- Isotopic evidence, *Science,* 256, 517-520, 1992.

Hanan, B.B., and D.W. Graham, Lead and helium isotope evidence from oceanic basalts for a common deep source of mantle plumes, *Science,* 272, 991-995, 1996.

Hanan, B.B., and Schilling, J.G., Easter microplate evolution: Pb isotope evidence, *J. Geophys. Res.,* 94, 7432-7448, 1989.

Hanan, B.B., Blichert-Toft, J., Pyle, D.G., and Christie, D.M., Contrasting origins or the upper mantle revealed by halfnium and lead isotopes from the Southeast Indian Ridge, *Nature*, 432, 91-94, 2004.

Hanan, B.B., Shervais, J.W., and Vetter, S.K., Yellowstone plume- continental lithosphere interaction beneath the Snake River Plain, *Geology*, 36, 51-54, 2008.

Hauri, E.H., J.A. Whitehead, and S.R. Hart, Fluid dynamic and geochemical aspects of entrainment in mantle plumes, *J. Geophys. Res.,* 99, 24275-24300, 1994.

Hofmann, A.W., Sampling mantle heterogeneity through oceanic basalts: Isotopes and trace elements, in *Treatise on Geochemistry: The Mantle and Core*, edited by Carlson, R.W., Holland, H.D., and Turekian, K.K., 61-101, 2003.

Horwitz, E.P., Dietz, M.L., Rhoads, S., Felinto, C., Gale, N.H., and Houghton, J., A lead-selective extraction chromatographic resin and its application to the isolation of lead from geological samples, *Analytica Chimica Acta,* 292, 263-2773, 1994.

Jackson, M.G., and Carlson, R.W., An ancient recipe for flood-basalt genesis, *Nature*,

476, 316-319, 2011.

Jackson, E.D., and Schlanger, S.O., Regional synthesis: Line Islands chain, Tuamotu Island chain, and Manihiki Plateau, central Pacific Ocean, *Initial Rep. Deep Sea Drill. Proj.,* 33, 915-927, 1976.

Konter, J.G., Hanan, B.B., Blichert-Toft, J., Koppers, A.A.P., Plank, T., and Staudigel, H., One hundred million years of mantle geochemical history suggest the retiring of mantle plumes is premature, *Earth Planet. Sci. Lett.,* 275, 285-295, 2008.

Korenaga, J., Why did not the Ontong Java Plateau form subaerially?, *Earth Planet. Sci. Lett.,* 234, 385-399, 2005.

Nakanishi, M., Tectonic evolution of the Mesozoic Pacific seafloor based upon magnetic anomaly lineations, D. Sc. Dissertation, 181 pp., the Univ. of Tokyo, Tokyo, 1991.

Nakanishi, M., and Sager, W.W., Formation of the Jurassic oceanic plateau, Shatsky Rise, northwestern Pacific Ocean, *Eos Trans. AGU*, 77 (46), 1996.

Nakanishi, M., and Winterer, E.L., Tectonic history of the Pacific-Farallon-Phoenix triple junction from Late Jurassic to Early Cretaceous: An abandoned Mesozoic spreading system in the Central Pacific Basin, *J. Geophys. Res.,* 103, 12453-12468, 1998.

Nakanishi, M., Tamaki, K., and Kobayashi, K., Mesozoic magnetic anomaly lineations and seafloor spreading history of the northwestern Pacific, *J. Geophys. Res.,* 94, 15437-15462, 1989.

Pin, C and Zalduegui, J.F.S., Sequential separation of light rare-earth elements, thorium and uranium by miniaturized extraction chromatography: Application to isotopic analyses of silicate rocks, *Analytica Chimica Acta*, 339, 79-89, 1997.

Rodriguez-Gonzalez, P., Monperrus, M., Garcia Alonso, J.I., Amouroux, D., and Donard, O.F.X., Comparison of different numerical approaches for multiple spiking species-specific isotope dilution analysis exemplified by the determination of butyltin species in sediments, *J. Anal. At. Spectrom.*, 22, 1373-1382, 2007.

Sager, W.W., What built Shatsky Rise, a mantle plume or ridge tectonics?, *in* Foulger, G.R., Natland, J.H., Presnall, D.C., and Anderson, D.L., *Plates, plumes and paradigms, Geol. Soc. Am. Spec. Paper,* 388, 721-733, 2005.

Schlanger, S.O., Jenkyns, H.C., and Premoli-Silva, I., Volcanism and vertical tectonics in the Pacific basin related to global Cretaceous transgressions, *Earth Planet. Sci. Lett.,* 52, 435-449, 1981.

Schubert, G., Masters, G., Olson, P., and Tackley, P., Superplumes or plume clusters?, *Physics Earth Planet. Int.,* 146, 147-162, 2004.

Steinberger, B., Plumes in a convecting mantle: models and observations for

individual hotspots, *J. Geophys. Res.,* 105, 11127-11152, 2000.

Stracke, A., Hofmann, A.W., and Hart, S.R., FOZO, HIMU and the rest of the mantle zoo, *Geochem. Geophys. Geosyst.,* 6, 1-20, 2005.

Tamaki, K., and Larson, R.L., The Mesozoic tectonic hstory of the Magellan microplate in the western central Pacific, *J. Geophys. Res.,* 93, 2857-2874, 1988.

Todt, W., Cliff, R.A., Hanse, A., and Hofmann, A.W., Evaluation of a 202Pb-205Pb double spike for high-precision lead isotopic analysis, *Geophys. Monograph,* 95, 429-437, 1996.

Torsvik, T.H., Steinberger, B., Cocks, L.R.M., and Burke, K., Longitude: Linking Earth's ancient surface to its deep interior, *Earth Planet. Sci. Lett.,* 276, 273-282, 2008.

Watts, A.B., Bodine, J.H., and Ribe, N.M., Observations of flexure and the geological evolution of the Pacific Ocean basin, *Nature*, 283, 532-537, 1980.

Wessel, P., Rooney, J., Hoeke, R., Weiss, J., Baker, J., Parrish, F., Fletcher, C. Chojnacki, J., Garcia, M.O., and Vroom, P., 2008, Geology and geomorphology of coral reefs of the Northwestern Hawaiian Islands, in *Coral Reefs of the USA*, edited by B. Riegl and R. E. Dodge, pp. 519-572, Springer Verlag, Berlin.

White, W.M., Albarede, F., and Telouk, P., High-precision analysis of Pb isotope ratios by multi-collector ICP-MS, *Chemical Geology*, 167, 257-270, 2000.

Winterer, E.L., Bathymetry and regional tectonic setting of the Line Islands Chain, *Initial Reports of the Deep Sea Drilling Project*, 33, 731-748, 1976.

Winterer, E.L., et al., *Initial Reports of the Deep Sea Drilling Project*, 17, 1973.

Zindler, A., and S. Hart, Chemical geodynamics, *Ann. Rec. Earth Planet. Sci.,* 14, 493-571, 1986.

Appendix

Sample Locations

A detailed bathymetric map was constructed to show the Line Islands volcanic chain, along with sample locations (Figure 4). Samples that were used in measuring isotopic ratios were plotted according to their latitude and longitude coordinates provided by Anthony Koppers.

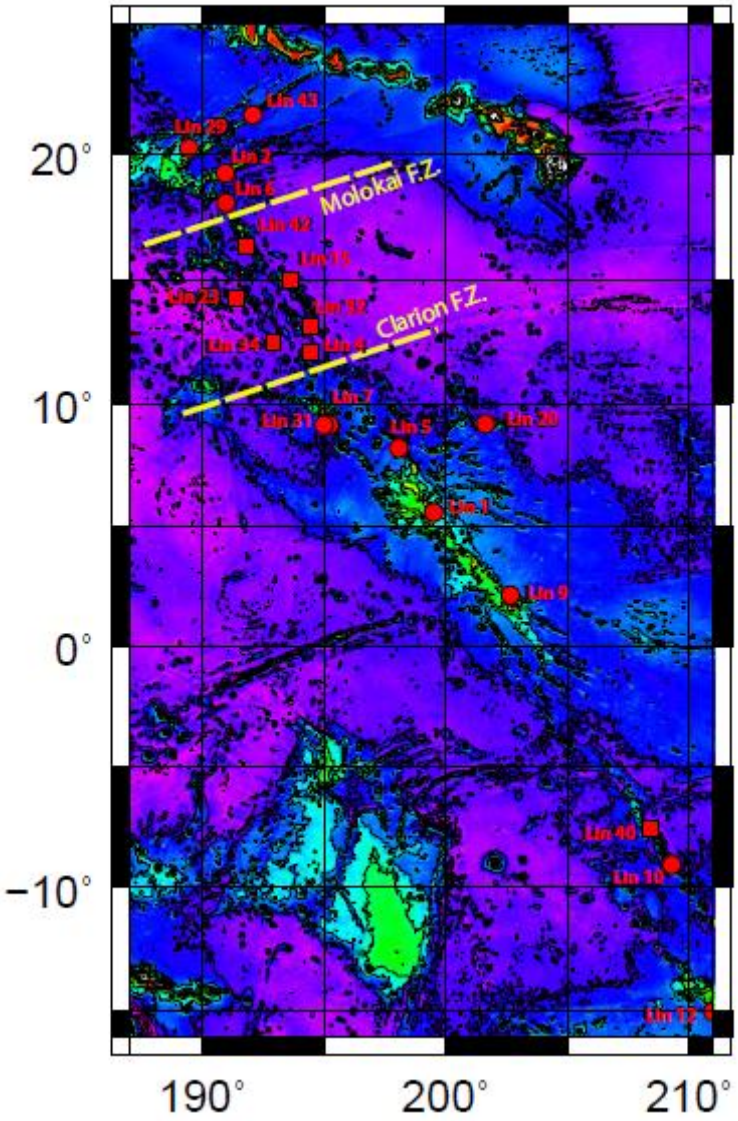

Figure 4: Bathymetric map of the Line Islands. Red squares represent samples with high $^{206}Pb/^{204}Pb$ ratios that lie within the Molokai and Clarion fracture zones. Red circles correspond to samples having average isotopic ratios following Hart et al, (1992), Hauri et al, (1994) and Hanan and Graham (1996).

Sample Descriptions and Isotope Data

In Figure 5, we provide a summary of the sample descriptions, represented by a Total Alkali and Silica (TAS) chart. Major and trace element geochemistry was measured at Michigan State University by Tyrone Rooney.

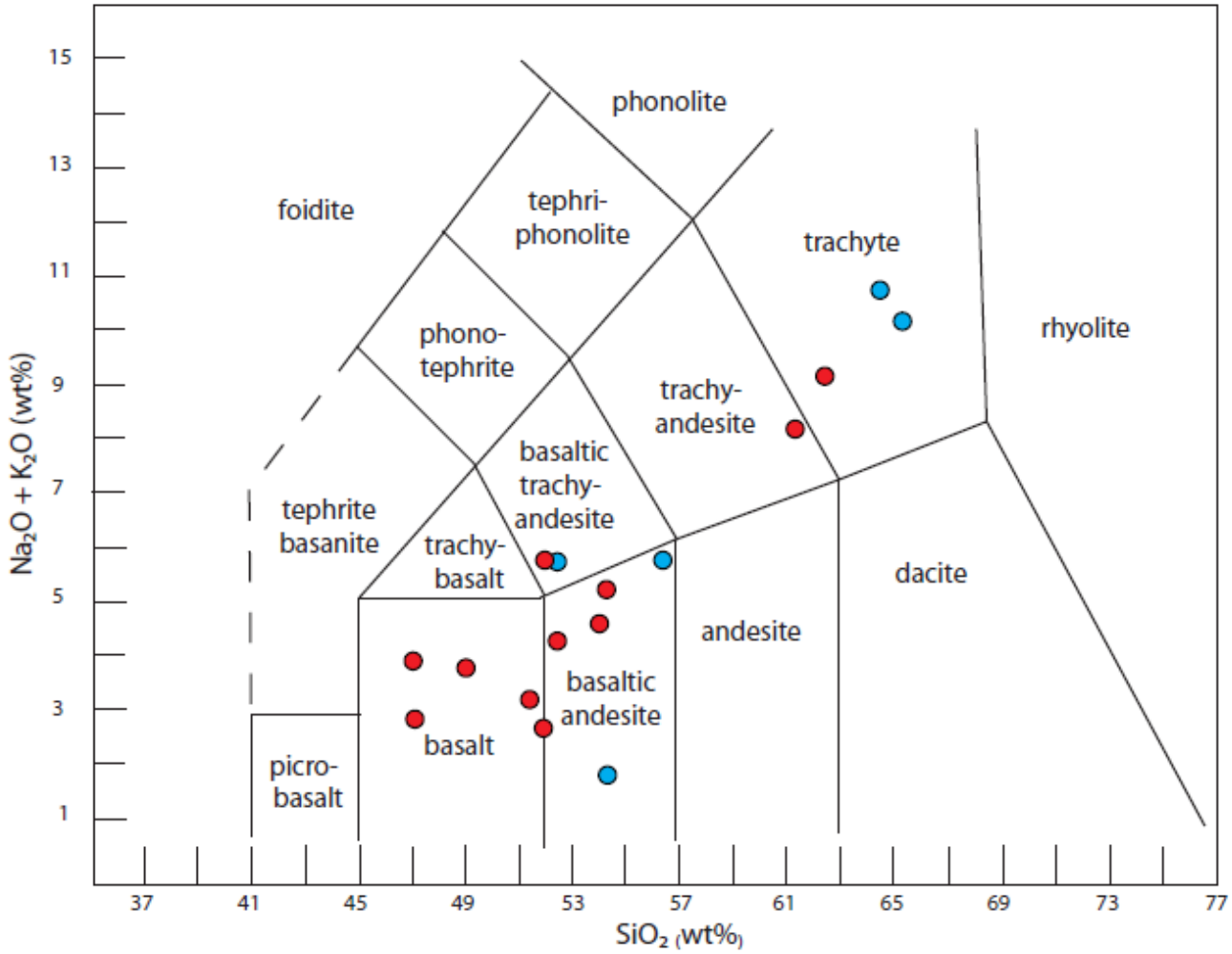

Figure 5: Total Alkali versus Silica chart. Sixteen samples were measured for major and trace elemental abundances, from which Na_2O, K_2O and SiO_2 weight percentages were used. Blue circles represent samples with high $^{206}Pb/^{204}Pb$ ratios that lie between the Molokai and Clarion fracture zones. Red circles correspond to average isotopic ratios following Hart et al, (1992), Hauri et al, (1994) and Hanan and Graham (1996).

In Table 1, a summary of our twenty new $^{87}Sr/^{86}Sr$, $^{208}Pb/^{204}Pb$, $^{207}Pb/^{204}Pb$, $^{206}Pb/^{204}Pb$ and $^{143}Nd/^{144}Nd$ is listed. Samples were dated using the $^{40}Ar/^{39}Ar$ dating technique at Oregon State University by Anthony Koppers. $^{87}Sr/^{86}Sr$ was normalized to SRM987 = 0.710248; Pb was normalized to NBS 981 ($^{208}Pb/^{204}Pb$ = 36.7006; $^{207}Pb/^{204}Pb$ = 15.4891; $^{206}Pb/^{204}Pb$ = 16.9356); $^{143}Nd/^{144}Nd$ was normalized to Jndi = 0.512116. Errors were measured at the 95% confidence level.

Sample	Latitude	Longitude	Age (Mya)	Error	$^{208}Pb/^{204}Pb$	2se	$^{207}Pb/^{204}Pb$	2se	$^{206}Pb/^{204}Pb$	2se	$^{87}Sr/^{86}Sr$	2se	$^{143}Nd/^{144}Nd$	2se
Lin1	5.52 N	160.51 W	83.0	1.1	39.087	9.5E-04	15.628	3.8E-04	19.209	4.9E-04	0.703851	3E-06	0.511839	8E-06
Lin2	19.25 N	169.05 W	94.2	1.3	38.965	1.4E-03	15.571	5.0E-04	19.206	6.0E-04	0.703772	5E-06	0.512958	8E-06
Lin4	12.04 N	165.50 W	93.3	0.7	39.418	1.5E-03	15.639	4.8E-04	19.788	5.2E-04	0.703680	5E-06	0.512947	2E-05
Lin5	8.18 N	161.92 W	38.4	1.1	39.060	8.6E-04	15.566	3.2E-04	19.268	4.0E-04	0.703275	3E-06	0.512834	2E-05
Lin6	18.08 N	169.04 W	94.1	0.9	39.595	1.2E-03	15.525	5.2E-04	19.113	6.0E-04	0.703586	4E-06	0.512969	1E-05
Lin7	9.08 N	164.73 W	67.6	0.9	39.311	3.1E-03	15.556	9.7E-03	19.472	8.3E-04	0.703644	1E-05	0.512928	5E-06
Lin9	2.10 N	157.35 W	36.2	0.4	38.626	1.8E-03	15.541	6.8E-04	19.063	8.1E-04	0.703654	7E-06	0.512870	5E-06
Lin10	9.07 S	150.70 W	75.5	0.9	38.721	1.2E-03	15.618	4.3E-04	19.048	4.3E-04	0.703194	3E-06	0.512871	5E-05
Lin12 G	15.02 S	149.03 W			38.944	5.1E-03	15.554	2.0E-03	19.354	1.8E-03	0.703131	3E-06	0.512980	1E-05
Lin12 P	15.02 S	149.03 W	54.3	0.8	38.857	4.6E-03	15.565	1.8E-03	19.263	2.1E-03	0.703096	4E-06	0.512878	3E-05
Lin15	14.98 N	166.45 W	84.0	0.8	39.775	1.8E-03	15.638	6.3E-04	20.149	8.3E-04	0.703089	3E-06	0.513002	3E-05
Lin20	9.18 N	158.38 W	80.5	1.0	38.983	2.2E-03	15.542	8.0E-04	19.128	7.6E-04	0.702986	4E-06	0.512872	2E-05
Lin23	14.27 N	168.59 W	70.9	0.5	40.509	1.5E-03	15.648	2.6E-04	20.052	6.4E-04	0.704312	4E-06	0.512881	9E-06
Lin29	20.22 N	170.57 W	75.9	0.7	38.602	1.4E-03	15.553	5.4E-04	18.881	6.2E-04	0.703577	4E-06	0.512905	1E-05
Lin31	9.14 N	164.78 W	69.2	0.8	39.012	1.4E-03	15.548	5.7E-04	19.265	6.3E-04	0.703447	4E-06	0.512898	7E-06
Lin32	13.15 N	165.49 W	88.8	0.8	40.119	1.2E-03	15.674	4.1E-04	19.822	4.9E-04	0.704610	3E-06	0.512801	2E-05
Lin34	12.52 N	167.05 W	97.8	0.7	40.059	1.7E-03	15.637	4.6E-04	19.871	5.3E-04	0.703535	3E-06	0.512746	5E-06
Lin40	7.58 S	151.55 W	66.9	1.3	39.203	5.3E-03	15.620	1.9E-03	19.827	2.6E-04	0.703804	2E-04	0.512966	4E-06
Lin42	16.45 N	168.22 W	83.0	1.8	40.110	3.7E-03	15.564	1.4E-03	19.876	1.8E-03	0.703110	3E-05	0.512916	9E-06
Lin43	21.53 N	167.93 W	89.7	0.8	38.484	7.7E-03	15.516	3.2E-04	18.747	3.9E-04	0.703112	5E-06	0.512961	2E-05

Table 1: Summary of ages and isotopic ratios from the Line Islands. Reported errors are at the 95% confidence level. Pb normalized to NBS981 ($^{208}Pb/^{204}Pb = 36.7006$; $^{207}Pb/^{204}Pb = 15.4891$; $^{206}Pb/^{204}Pb = 16.9356$); Sr normalized to SRM987 ($^{87}Sr/^{86}Sr = 0.710248$; Nd normalized to Jndi ($^{143}Nd/^{144}Nd = 0.512116$).

Vita

Lauren P. Storm was born in Spring Grove, Pennsylvania; the third child of Lynne Small and Christopher Storm. She graduated from Spring Grove Area High School in the spring of 2006, and graduated from Kutztown University of Pennsylvania with a bachelor's degree in Geology in the spring of 2010. While attending Kutztown University, Lauren had the opportunity to conduct research in south-central Utah, for which she is a corresponding author on three papers entitled "Growth faults in the Kaiparowits Basin, Utah, pinpoint initial Laramide deformation in the western Colorado Plateau," "Predatory digging behavior by dinosaurs," and "Attributes of the wood-bearing trace fossil *Asthenopodichnium* in the Late Cretaceous Wahweap Formation, Utah, USA." A research assignment during her Sedimentology/Stratigraphy class also landed her a first author paper entitled "Large Vertebrate Burrow from the Upper Mississippian Mauch Chunk Formation, Eastern Pennsylvania, USA." Lauren moved to El Paso, Texas in the summer of 2012 to pursue her master's in Geology.

Permanent address: 4111 Westcity Ct #78
El Paso, TX 79902
lpstorm@miners.utep.edu

This thesis was typed by the author.